International Journal of Applied Earth Observations and Geoinformation 94 (2021) 102238

Contents lists available at ScienceDirect

International Journal of Applied Earth Observations and Geoinformation

journal homepage: www.elsevier.com/locate/jag

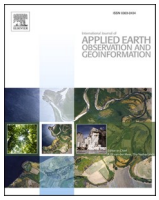

Global trends in vegetation seasonality in the GIMMS NDVI3g and their robustness

Wentao Ye [a,*], Albert I.J.M. van Dijk [a], Alfredo Huete [b], Marta Yebra [a,c]

[a] Fenner School of Environment & Society, Australian National University, Canberra, Australia
[b] School of Life Sciences, University of Technology Sydney, Sydney, Australia
[c] Research School of Aerospace, Mechanical, and Environmental Engineering, Australian National University, Canberra, Australia

ARTICLE INFO

Keywords:
Vegetation seasonality
NDVI
Trend analysis
Robustness
NDVI3g
MODIS

ABSTRACT

Analysing changes in vegetation seasonality of terrestrial ecosystems is important to understand ecological responses to global change. Based on over three decades of observations by the series of Advanced Very High Resolution Radiometer (AVHRR) sensors, the Global Inventory Modelling and Mapping Studies (GIMMS) Normalized Difference Vegetation Index (NDVI) dataset has been widely used for monitoring vegetation trends. However, it is not well known how robust long-term trends in vegetation seasonality derived from GIMMS NDVI are, given inevitable influences from sensor and processing artefacts. Here we analyse long-term seasonality trends in the GIMMS third generation (NDVI3g) record (1982–2013). Changes in vegetation seasonality are decomposed into changes in duration (related to growing season length) and timing (related to peak growing season). We compare seasonality trends from the previous version (NDVI3g v0) with those in the subsequently released version (NDVI3g v1) and, for their common period, with those derived from MODerate Resolution Imaging Spectroradiometer (MODIS) collection 6 NDVI. We find that NDVI3g v0 shows marked seasonality trends for 1982–2013 over more than one-third of the global vegetated area. Long-term trends based on v1 are generally consistent with v0, but v1 shows a strong trend towards earlier timing across the Arctic regions that is absent in v0. NDVI3g v0, v1, and MODIS all point towards an increased duration across the tundra of North Asia and later timing across North Africa. However, several discrepancies are also found between the NDVI datasets. For example, for the North-American tundra, MODIS shows earlier and v0 later timing, while MODIS shows an increased duration and v1 a reduced duration. For North Africa, v0 and v1 exhibit a reduced duration that is absent in MODIS. We conclude that both the primary observations and the subsequent processing can have a marked influence on inferred seasonality trends, and propose that the robustness of trends should be examined and corroborated using alternative data sources wherever possible.

1. Introduction

Vegetation seasonality can be defined as the occurrence of periodical intra-annual patterns in vegetation structure or function (e.g., leaf area, photosynthesis) and is not identical, but closely related to phenology (Eastman et al., 2013; Guan, 2013). Identifying shifts in vegetation seasonality from satellite observations offers the opportunity to understand the impacts of natural and human-induced processes on terrestrial ecosystems at large-scales (Park et al., 2019; Wang et al., 2019a; Xu et al., 2013). As a remotely sensed proxy of vegetation cover or photosynthetic capacity, the Normalized Difference Vegetation Index (NDVI) (Tucker, 1979) is widely used for monitoring terrestrial vegetation activity (De Jong et al., 2013; Myneni et al., 1997; Piao et al., 2011; Zhou et al., 2001), and seasonal NDVI time series are well-suited to describing vegetation seasonality. Shifts in vegetation seasonality can be quantified by changes in duration and timing of seasonal NDVI activity, respectively (Buitenwerf et al., 2015; Garonna et al., 2016; Gonsamo et al., 2018).

Based on a series of Advanced Very High Resolution Radiometer (AVHRR) sensors, global NDVI datasets have been generated to analyse vegetation dynamics over the three decades. Among different AVHRR-based NDVI datasets, the Global Inventory Modelling and Mapping Studies (GIMMS) NDVI has been shown to have the highest temporal consistency (Tian et al., 2015), including for trend analyses (Beck et al.,

* Corresponding author.
E-mail address: wentao.ye@anu.edu.au (W. Ye).

https://doi.org/10.1016/j.jag.2020.102238
Received 30 April 2020; Received in revised form 28 August 2020; Accepted 10 September 2020
Available online 19 September 2020

2011; Marshall et al., 2016). Based on the latest (third) generation of GIMMS NDVI (NDVI3g), long-term (>30 years) trends in vegetation seasonality or phenology have been reported at continental and global scales (Buitenwerf et al., 2015; Eastman et al., 2013; Garonna et al., 2014, 2016; Xu et al., 2013).

Due to the uniquely long AVHRR record, long-term vegetation trends inferred from GIMMS data have typically been reported without examining their robustness using alternative data. Although the GIMMS data have been corrected for issues such as orbital drift, sensor degradation, and platform/sensor changes (Pinzon and Tucker, 2014; Tucker et al., 2005), a previous study has identified remaining artefacts in the NDVI time series (Tian et al., 2015), which may affect trend analyses. A few studies have revealed inconsistencies of trends in vegetation dynamics between GIMMS NDVI and other independent sources (Alcaraz-Segura et al., 2010; Kern et al., 2016; Scheftic et al., 2014; Yin et al., 2012; Zhang et al., 2013). For example, Alcaraz-Segura et al. (2010) reported that GIMMS failed to capture post-fire NDVI recovery in the North American boreal forests compared with another dataset (AVHRR 1 km) from the Canadian Centre for Remote Sensing (Latifovic et al., 2005). Zhang et al. (2013) found that the GIMMS-based trends in the start of growing season over the Tibetan Plateau after 2001 substantially differed from those from MODIS (MODerate Resolution Imaging Spectroradiometer) and SPOT-VGT (Système Pour l'Observation de la Terre VEGETATION). These studies suggest the importance of evaluating the robustness of long-term trends in vegetation dynamics detected only using the GIMMS NDVI. GIMMS-based trends in greenness have been evaluated at regional and global scales with other satellite observations using common periods (Fensholt and Proud, 2012; Fensholt et al., 2009; Guay et al., 2014; Jiang et al., 2017). However, to our knowledge, no attempt has been made to evaluate how robust the global trends in vegetation seasonality derived from GIMMS NDVI compared to those from alternative NDVI datasets.

In this study, we aimed to investigate long-term trends in vegetation seasonality globally and evaluate the robustness of trends derived from the NDVI3g record. First, we analysed long-term seasonality trends and identified regions where significant trends occur over the three decades. Subsequently, for these regions, we evaluated the consistency of seasonality trends between the NDVI3g and alternative NDVI data for their common data periods.

2. Data and methods

2.1. NDVI datasets

We used two versions of GIMMS NDVI3g (Pinzon and Tucker, 2014) for the period 1982–2013, version 0 (v0) and a more recent version 1 (v1) that maintains the main features of v0 (Pinzon, 2017, pers. comm.) but extends the record to 2015. We used v0 as our reference because most studies on vegetation dynamics published to date were based on v0, even in more recent years (Buermann et al., 2018; Huang et al., 2018, 2017; Pan et al., 2018). To test for consistency in seasonality trends, we compared the trends found in v0 with v1 for 1982–2013. The NDVI data were generated every 15 days at 1/12° spatial resolution. We aggregated the biweekly data into monthly values using maximum value compositing (Holben, 1986). We used the latest version of MODIS NDVI (Collection 6 or C6) to compare seasonality trends with NDVI3g for their common period (2001–2013). The NDVI data were generated monthly at 0.05° spatial resolution.

2.2. Global vegetation biome map

The MODIS IGBP (International Geosphere-Biosphere Programme) land cover map (Friedl et al., 2010) and a revised map of the Köppen-Geiger climate zones (Beck et al., 2016) (http://www.gloh2o.org/other/) were combined to map seven broad biomes (i.e., tropical forests, extra-tropical forests, savannahs, grasslands, croplands, shrublands, and tundra) as follows (Fig. 1). Forests in tropical regions were classified as tropical forests and in other climate regions as extra-tropical forests. The MODIS land cover dataset shows some woody savannas in cold regions, which were interpreted as classification errors and reclassified as extra-tropical forests. Savannahs in tropical regions were merged with woody savannahs, and in other climate regions are merged with grasslands. Based on the MODIS land cover map, the category 'shrubland' includes both closed and open shrublands and the category 'cropland' includes both 'croplands' and 'cropland/natural vegetation mosaic'. A new category 'tundra' includes grasslands and shrublands in polar regions and cold regions with a cold summer or very cold winter. Other land surface types were considered to have no vegetation.

2.3. Definition of a phenological year

The timing of climatic constraints (e.g., precipitation or temperature) to vegetation growth varies between regions and NDVI seasonality within a calendar year (January to December) does not always align with a typical cycle of vegetation growth (e.g., from dormancy via green-up to peak growth and back via senescence). To define the 12-month period that best encompasses the cycle, for each pixel we first determined the month for which maximum NDVI occurs in the long-term averaged monthly values (Fig. 2a). We then define the phenological year as starting six months before the peak month until five months thereafter, for the purpose of calculating annual seasonality metrics. We exclude vegetated areas with bimodal or multimodal NDVI seasonality from the analysis. Such areas were identified by two criteria: (1) there are two or more peaks in the average monthly NDVI pattern, and (2) the NDVI values of the first and second largest peaks both exceed mean NDVI. Examples include regions encompassing African rainforests, Indian croplands, and Australian shrublands (Fig. 2b-d).

2.4. Detecting trends in vegetation seasonality

We characterised changes in vegetation seasonality in two dimensions: the change in duration (or concentration of NDVI distribution) and the change in timing (Fig. 3). The metrics describing duration and timing are based on the framework proposed by Feng et al. (2013). For a phenological year, we first normalize the monthly NDVI by the sum of NDVI over the year. The result can be interpreted as a discrete probability distribution (denoted as p_m for each month m). In some areas (mainly in the tundra), there are negative NDVI values due to snow and ice cover. These values are computationally meaningless when calculating the discrete probability distribution and generally assumed ecologically meaningless for analysing vegetation dynamics (Zhang et al., 2017). To minimise the effects of snow/ice, we replaced negative NDVI with zero before normalisation. We then use the entropy (R) and centroid (C) of p_m as measures of duration and timing, respectively:

$$R = -\sum_{m=1}^{12} p_m \log_2(p_m) \quad (1)$$

$$C = \sum_{m=1}^{12} m \cdot p_m \quad (2)$$

Changes in entropy and centroid can be linked to changes in seasonality (Fig. 3). A decrease in entropy suggests more concentrated seasonality (reduced duration), while an increase suggests less concentrated seasonality (increased duration). A decrease in the centroid suggests a change towards timing earlier in the phenological year, while an increase suggests a later timing. To detect trends in seasonality, we apply linear regression to the time series of the entropy and the centroid for each grid cell. The statistical significance of trends was determined using the Mann–Kendall trend test at $p < 0.05$. It is noted that seasonality trends in our analysis are not intended to serve as measures of

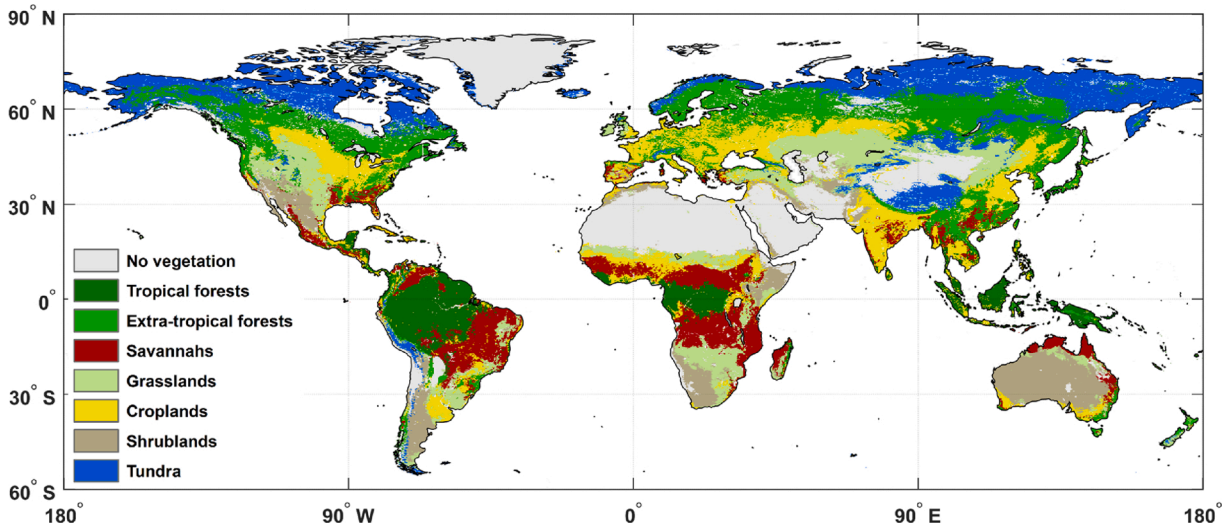

Fig. 1. Global vegetation biome map with eight classes based on the MODIS IGBP land cover map and the Köppen-Geiger climate classification map.

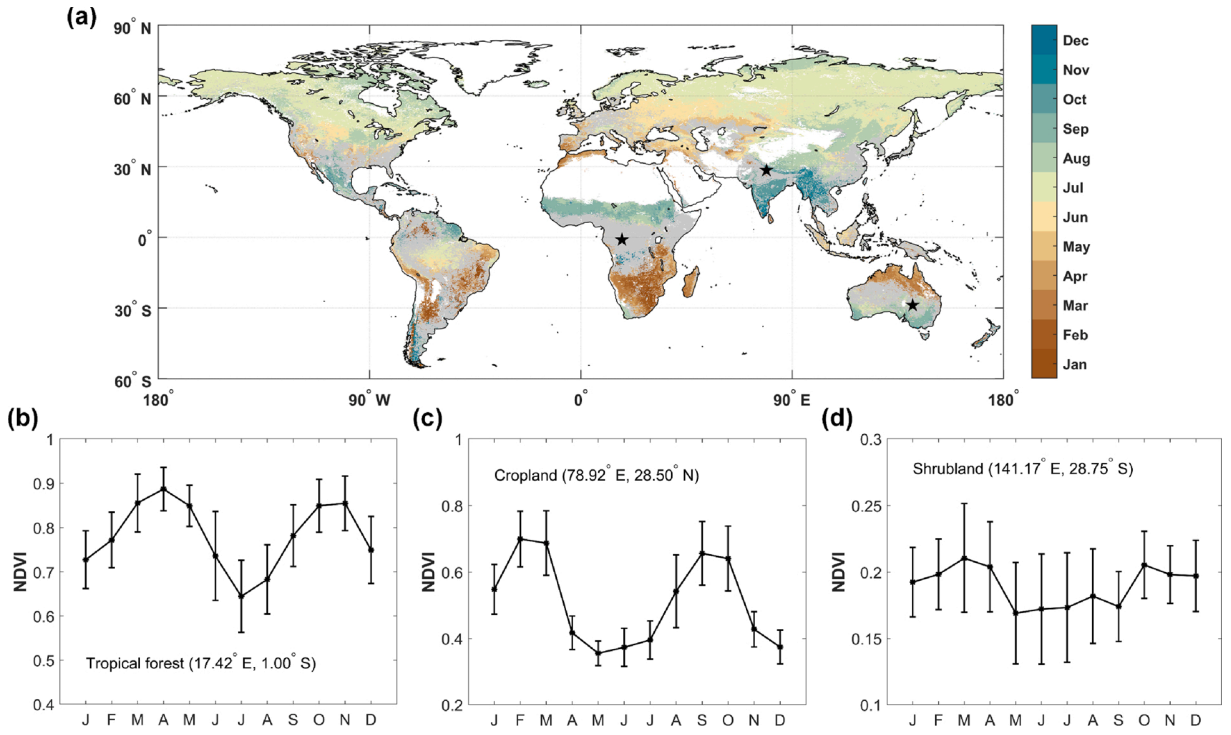

Fig. 2. Timing of vegetation peak growth. (a) Global distribution of peak timing. Areas without vegetation are masked white and areas with bi- or multimodal NDVI seasonality are shaded grey. (b-d) Average seasonal NDVI pattern for three locations with a bimodal seasonality indicated by the black stars in (a). The curve and error bars are mean and standard deviation of the monthly NDVI for 1982–2013.

changes in specific phenological events (e.g, growing season length or peak season) given difficulties of identifying phenological change using satellite observations (Eastman et al., 2013; Helman, 2018). However, interpretations of seasonality trends will typically still be consistent with changes in land surface phenology reported by previous studies, which will be discussed.

3. Results

3.1. Trends in vegetation seasonality from 1982 to 2013

NDVI3g v0 showed significant seasonality trends for 1982–2013 over more than one-third of the global vegetated area (Fig. 4). About 29 % and 14 % of vegetated lands exhibit significant trends in duration (i.e., entropy) and timing (i.e., centroid), respectively (Fig. 4a,b). Several spatial clusters can be identified (Fig. 4c). The North-American tundra showed an increased duration (mean +0.0019 per year (y^{-1}) trend in entropy) and a slightly later timing (mean +0.0023 month per year trend in centroid timing), which can be converted to units of 'days per decade' by multiplying by 305 (~30.5 days per month and 10 years per decade) to yield ca. + 0.7 days per decade. The North-Asian tundra exhibited a stronger increase in duration (mean +0.0041 y^{-1}) compared with the North-America tundra but did not show a clear trend in timing. Central Asia exhibited a reduced duration (mean −0.0035 y^{-1}), accompanied by a later timing (mean +1.1 days per decade). Seasonality trends in the forests of East Asia showed a reduction in duration (mean

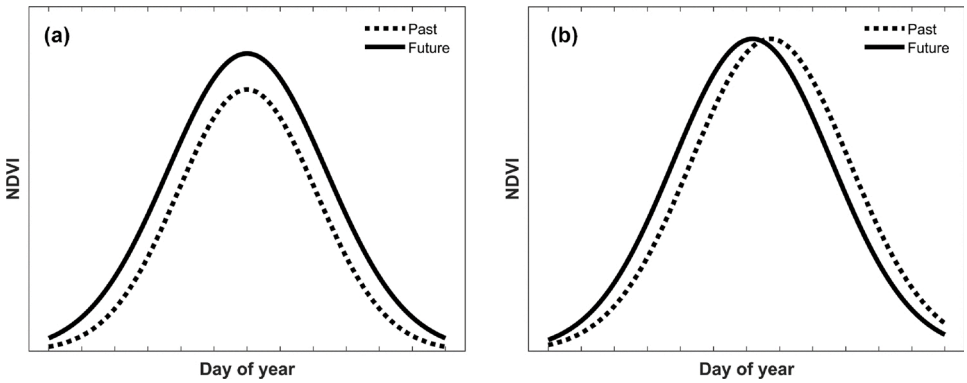

Fig. 3. Conceptual diagrams illustrating changes in vegetation seasonality. (a) Change in duration: the scenario shows a trend towards higher entropy and a longer growing season as NDVI becomes less temporally concentrated. (b) Change in timing: the scenario shows a trend towards earlier timing of growth as the NDVI centroid moves forward in the year.

$-0.0023\ y^{-1}$) and a slight delay in timing (mean +0.5 days per decade). North Africa showed a greater delay in timing (mean +1.5 days per decade) compared to other regions as well as a small reduction in duration (mean $-0.001\ y^{-1}$). The drylands of southern Africa and the savannahs of northern Australia also exhibited a slightly reduced duration (Fig. 4a,c).

3.2. Comparison of seasonality trends between NDVI datasets

We compared seasonality trends between pairs of datasets for the five identified regions (Fig. 4c): the tundra of North American and North Asia, the drylands and savannahs of North Africa, the grasslands, and croplands of Central Asia, and the forests of East Asia. For each region, two datasets are expected to show a similar probability distribution of trends in both entropy and centroid for their common period. We performed the comparison at the regional level rather than the pixel level for two reasons. First, the seasonality trend of a single pixel can be easily influenced by the uncertainties (e.g., cloud contamination or atmospheric correction) in the datasets. Comparing probability distributions for an identified region helps avoid random bias or errors in seasonality trends at the pixel level. Second, it allows a comparison without resampling MODIS to the same spatial resolution as NDVI3g. We applied the mask of identified regions (Fig. S1) to each dataset, respectively.

We first compared seasonality trends between NDVI3g v0 and v1 for 1982–2013. We found their long-term trends were highly consistent among the five clusters except for the tundra regions (Fig. 5). In particular, v1 showed an advance in timing (mean −1.7 days per decade) across the Arctic tundra, which contradicts the slightly delayed timing found in v0.

We further compared seasonality trends between NDVI3g v0 and MODIS NDVI for the period 2001–2013. We found discrepancies in duration or timing trends between the two datasets for all five regions (Fig. 6). For the North-American tundra, MODIS showed earlier timing (mean −1.0 days per decade), whereas v0 showed later timing (mean +2.8 days per decade). For the North-Asia tundra, MODIS showed an advance in timing (mean −2.0 days per decade) while v0 showed a delay (mean +1.9 days per decade). In Central Asia, MODIS exhibits an increase in duration (mean $+0.0031\ y^{-1}$) whereas v0 exhibits a reduction (mean $-0.0025\ y^{-1}$). Moreover, MODIS showed later timing (mean +2.5 days per decade) whereas v0 did not show any clear trend. For the forests of East Asia, MODIS did not show any clear trend in duration while v0 showed a reduction ($-0.0031\ y^{-1}$). For North Africa, MODIS did not exhibit any clear trend in duration whereas v0 showed a reduced duration (mean $-0.0026\ y^{-1}$).

We also compared seasonality trends between NDVI3g v1 and MODIS NDVI for the period 2001–2013. Overall, v1 showed more consistency with MODIS than v0 (Fig. S2). The discrepancies in trends in timing between MODIS and v0 in the Arctic regions were not found between MODIS and v1; both showed a trend towards earlier timing. However, considerable inconsistencies remained. For the North-American tundra, the mean trend in duration of v1 ($+0.0011\ y^{-1}$) was only a tenth of that of MODIS ($+0.011\ y^{-1}$). For the North-Asian tundra, the mean trend in timing of v1 (−8.0 days per decade) was four times that of MODIS (−2.0 days per decade). For Central Asia, the discrepancies in trends in duration between MODIS and v0 did not occur between MODIS and v1, but v1 showed a slightly earlier timing (−0.9 days per decade) compared to a delayed timing in MODIS (mean +2.5 days per decade). For North Africa, v1 exhibited a reduced duration (mean $-0.0012\ y^{-1}$) that was absent in MODIS.

4. Discussion

All three NDVI datasets pointed towards an increased duration across the tundra of North Asia (Fig. 6 and Fig. S2), suggesting a lengthening of the growing season that has previously been attributed to Arctic warming (Keenan and Riley, 2018). The three datasets also showed fairly consistent later timing across North Africa, probably explained by a delay in start or end of season as indicated by a recent study using vegetation optical depth derived from long-term passive microwave observations (Tong et al., 2019).

Beyond these robust seasonality trends, our analysis also indicates several inconsistencies between NDVI3g and MODIS. The AVHRR sensor has a wider red (0.58–0.68 μm) and near-infrared (NIR, 0.73–1.1 μm) bandwidth than MODIS (0.62–0.67 μm for the red band and 0.841–0.876 μm for the NIR band). In the red band, AVHRR NDVI has an extended range of chlorophyll sensitivity from low to high greenness states, which may lead to changes in the shape of a seasonal profile compared to MODIS NDVI. A previous study proposed a method to convert MODIS NDVI to "AVHRR-like" NDVI using a linear combination of MODIS green and red bands instead of the red band (Gitelson and Kaufman, 1998). However, Miura et al. (2006) found that it did not help to reduce overall inconsistencies between MODIS and AVHRR NDVI. This suggests that the wider red band does not explain the discrepancies in seasonality trends between NDVI3g and MODIS found here. In the NIR band, the wider AVHRR band encompasses some major water absorption features (e.g., 0.81 to 0.84 μm), while MODIS NIR was purposefully designed to avoid those absorption regions. Atmospheric humidity (water vapor content) may impact AVHRR NIR and lead to lower NDVI. As AVHRR NDVI is not atmospherically corrected (Tian et al., 2015), it is feasible that water vapor effects could shift seasonal NDVI profile and thereby the seasonality metrics, resulting in the observed inconsistencies.

Our analysis also indicates that the processing of the observations can have an important influence on subsequent trend analyses. The

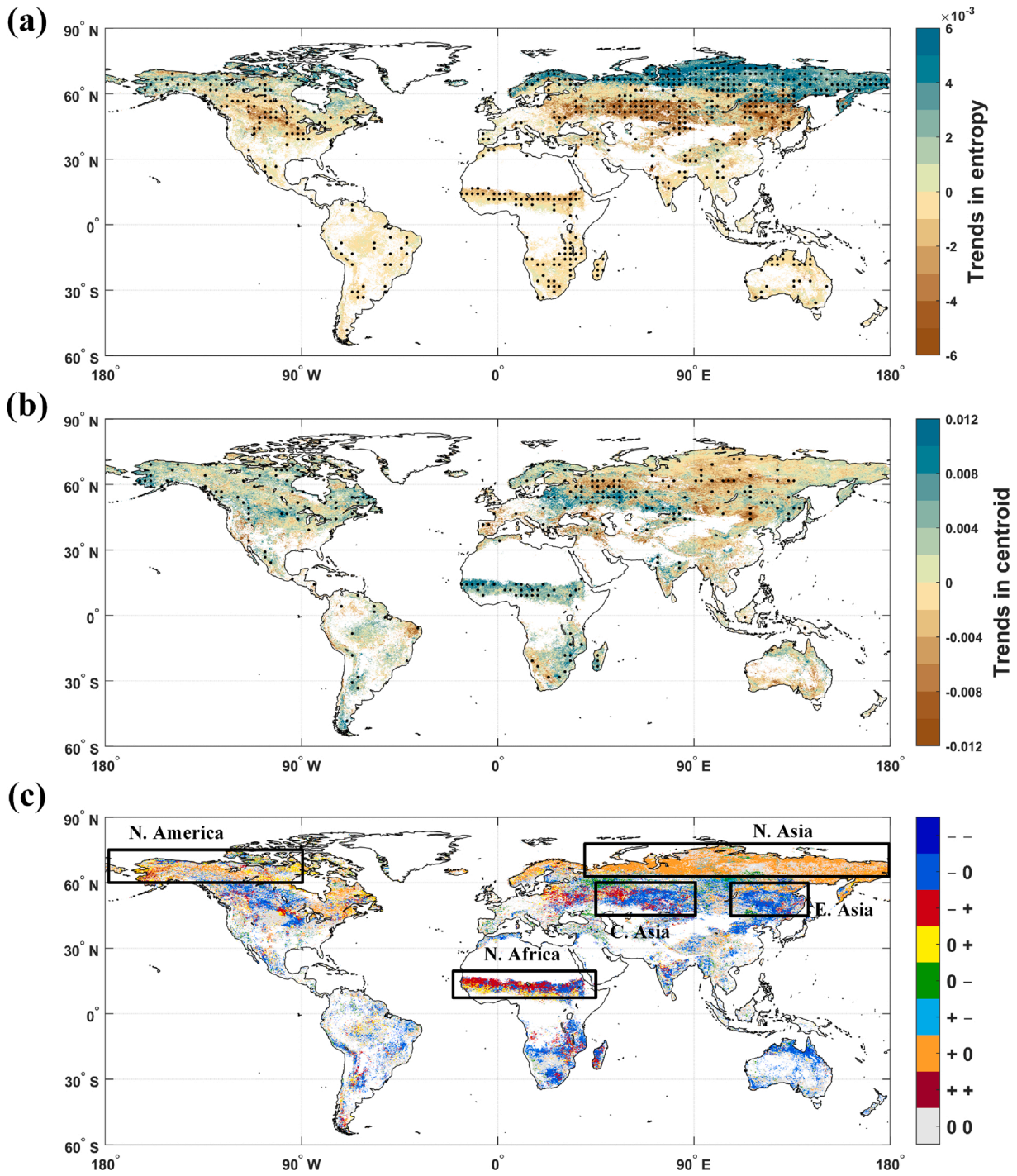

Fig. 4. Trends in vegetation seasonality for the period 1982–2013 based on NDVI3g v0. Global distribution of trends in (a) NDVI entropy and (b) NDVI centroid. Areas without vegetation or with bi- or multimodal seasonality are masked white. Black dots indicate statistically significant trends at $p < 0.05$. (c) Global distribution of ecosystems where significant trends in entropy or centroid are found. The label '+', '−' or '0' represents significant positive trends, significant negative trends or no significant trends, respectively. For example, '+ −' represents areas with a significant positive trend in entropy and a significant negative trend in centroid timing. The black rectangles highlight five identified clusters discussed in the text.

earlier timing across the tundra observed in MODIS was consistent with the advance in peak photosynthetic activity reported by a recent study (Park et al., 2019), but NDVI3g v0 did not show such a trend or even an opposite trend. This difference appears to be reduced in the more recent NDVI3g v1, possibly because v1 has addressed calibration issues that existed in v0 (Burrell et al., 2018). Previous evaluations (e.g., Beck et al., 2011) demonstrated that MODIS observations and derived NDVI record have better accuracy than those from AVHRR, as would be expected based on the more advanced sensor and mission design. Given the discrepancies in seasonality trends between NDVI3g v1 and MODIS for some regions (e.g., the North-American tundra and Central Asia), caution would seem advisable when using v1 to investigate trends in vegetation dynamics in these regions.

In addition to NDVI3g, there are several of the NDVI datasets available for monitoring global vegetation dynamics over more than three decades. One of them is the Land Long Term Data Record (LTDR)

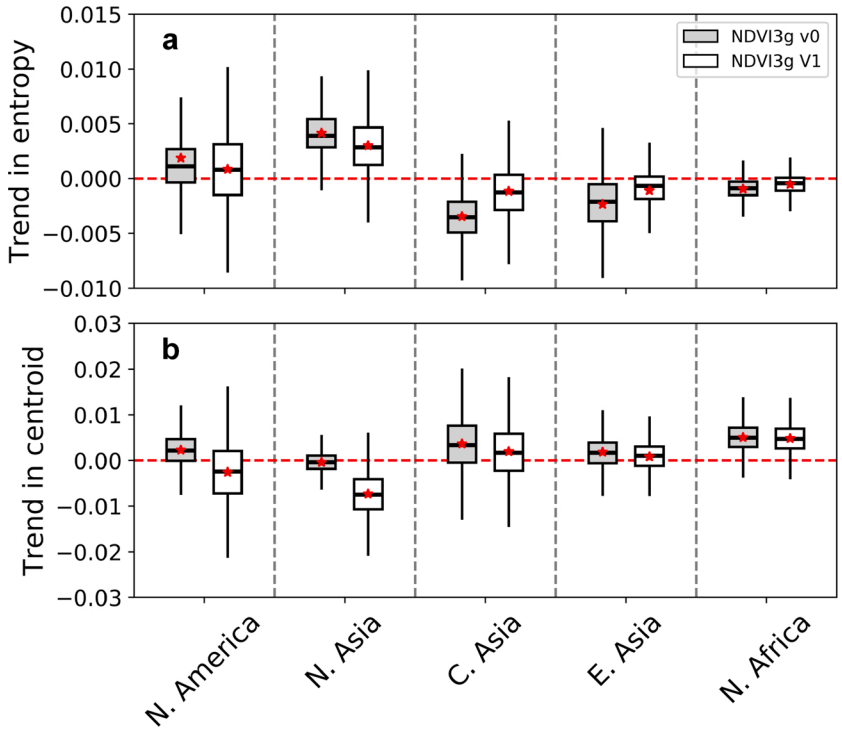

Fig. 5. Box plots comparing NDVI3 v0 and v1 derived trends in (a) entropy and (b) centroid timing for the five cluster regions and the common period 1982–2013 (Fig. 4c). Red stars indicate mean values.

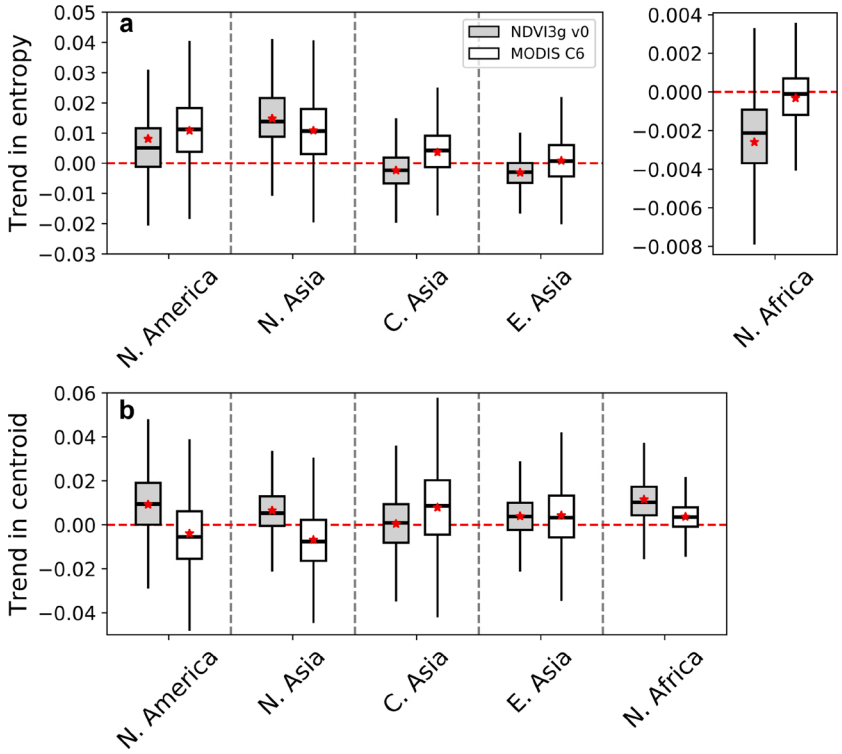

Fig. 6. Box plots comparing NDVI3 v0 and MODIS C6 NDVI derived trends in (a) entropy and (b) centroid timing for the five cluster regions and the common period 2001–2013 (Fig. 4c). Red stars indicate mean values.

derived from AVHRR surface reflectance (1981–present) with significant efforts to improve calibration, geolocation accuracy, and cloud masking (Franch et al., 2017; Villaescusa-Nadal et al., 2019). Another alternative is the Vegetation Index and Phenology (VIP) dataset merging LTDR (1981–1999) and MODIS record (2000–2014) (Didan and Barreto, 2016). Although both datasets received greater attention to atmospheric effects when compared with NDVI3g, their performance in trend analysis has been reported to be worse than the latter, apparently due to a lack of temporal consistency (Marshall et al., 2016; Tian et al., 2015). It is noted that these comparisons have used earlier releases of the

respective datasets. More recently released versions may show improved performance. Nevertheless, it remains uncertain how potential artefacts (Tian et al., 2015) may influence seasonality trends, and without further evidence, NDVI3g v1 may still be considered the best choice for long-term trend analysis at present (Burrell et al., 2018).

Despite ending in 2013 (v0) or 2015 (v1), NDVI3g has continued to be used in studies in recent years (Fig. S3). Some recent studies report changes in land surface phenology at large scales (global or hemispheric) based on NDVI3g (Buitenwerf et al., 2015; Garonna et al., 2016; Gonsamo et al., 2018; Wang et al., 2015, 2019b) and such changes may be related to seasonality trends calculated here. For example, the increased duration in the Arctic regions (Fig. 4a) is consistent with longer growing seasons found by Buitenwerf et al. (2015). In contrast, Garonna et al. (2016) reported a shortening of growing season length (GSL) across the Pan-Arctic region. Both studies were solely based on NDVI3g v0, and therefore, changes in Arctic GSL may need to be revisited. In addition, a widespread advance in timing in the northern hemisphere (Fig. S4) is consistent with the shift of the vegetation peak season towards spring reported by Gonsamo et al. (2018). Their study also found a persistent advance of the start of growing season (SOS) in the northern hemisphere during 1982–2015, whereas Wang et al. (2019b) reported a hiatus of the SOS advancing during 1998–2012 based on the same NDVI3g v1. Given the disagreement between previous studies and the discrepancies in seasonality trends between NDVI datasets found here, the robustness of trends in spring and autumn phenology in the northern ecosystems may need to be examined further.

5. Conclusions

We investigated long-term trends in vegetation seasonality based on GIMMS NDVI3g. We found that NDVI3g v0 showed marked seasonality trends over large parts of the global vegetated lands for the period 1982–2013. Comparisons between NDVI3g v0 and the more recent version v1 and MODIS C6 NDVI data revealed both consistencies and inconsistencies in seasonality trends. The existence of inconsistencies between NDVI products complicates a reliable assessment of changing vegetation dynamics, with results and interpretation contingent on the choice of NDVI products. Inconsistencies between product versions derived from the same sensor also suggest that the processing of the original observations can have a significant impact on subsequent trend analyses. Evaluating the robustness of the results with alternative NDVI datasets or relevant observations where available would be desirable to ensure that detected trends reflect true seasonality trends rather than artefacts originating from the sensor observations or processing methods.

CRediT authorship contribution statement

Wentao Ye: Conceptualization, Methodology, Formal analysis, Investigation, Writing - Original draft. **Albert I.J.M. van Dijk**: Conceptualization, Writing - Review & editing, Supervision. **Alfredo Huete**: Writing - Review & editing, Supervision. **Marta Yebra**: Writing - Review & editing, Supervision.

Declaration of Competing Interest

The authors declare that they have no known competing financial interests or personal relationships that could have appeared to influence the work reported in this paper.

Acknowledgments

This research was supported by the Australian Research Council's Discovery ProjectDP140103679. We thank NASA Earth Exchange (NEX) platform for providing NDVI3g v0 and v1, and NASA's Land Processes Distributed Active Archive Centre (LP DAAC) for providing MODIS Terra C6. We thank GLCF (http://glcf.umd.edu) and GLOH2O (http://www.gloh2o.org/) for providing the MODIS IGBP land cover map and the Köppen − Geiger climate classification map, respectively.

Appendix A. Supplementary data

Supplementary material related to this article can be found, in the online version, at doi:https://doi.org/10.1016/j.jag.2020.102238.

References

Alcaraz-Segura, D., Chuvieco, E., Epstein, H.E., Kasischke, E.S., Trishchenko, A., 2010. Debating the greening vs. browning of the North American boreal forest: differences between satellite datasets. Glob. Chang. Biol. 16, 760–770.
Beck, H.E., McVicar, T.R., van Dijk, A.I., Schellekens, J., de Jeu, R.A., Bruijnzeel, L.A., 2011. Global evaluation of four AVHRR–NDVI data sets: intercomparison and assessment against Landsat imagery. Remote Sens. Environ. 115, 2547–2563.
Beck, H.E., van Dijk, A.I., de Roo, A., Miralles, D.G., McVicar, T.R., Schellekens, J., Bruijnzeel, L.A., 2016. Global-scale regionalization of hydrologic model parameters. Water Resour. Res. 52, 3599–3622.
Buermann, W., Forkel, M., O'Sullivan, M., Sitch, S., Friedlingstein, P., Haverd, V., Jain, A.K., Kato, E., Kautz, M., Lienert, S., 2018. Widespread seasonal compensation effects of spring warming on northern plant productivity. Nature 562, 110–114.
Buitenwerf, R., Rose, L., Higgins, S.I., 2015. Three decades of multi-dimensional change in global leaf phenology. Nat. Clim. Chang. 5, 364–368.
Burrell, A.L., Evans, J.P., Liu, Y., 2018. The impact of dataset selection on land degradation assessment. ISPRS J. Photogramm. Remote. Sens. 146, 22–37.
De Jong, R., Schaepman, M.E., Furrer, R., Bruin, S., Verburg, P.H., 2013. Spatial relationship between climatologies and changes in global vegetation activity. Glob. Chang. Biol. 19, 1953–1964.
Didan, K., Barreto, A., 2016. NASA MEaSUREs Vegetation Index and Phenology (VIP) Vegetation Indices Daily Global 0.05Deg CMG. NASA EOSDIS Land Processes DAAC.
Eastman, J.R., Sangermano, F., Machado, E.A., Rogan, J., Anyamba, A., 2013. Global trends in seasonality of normalized difference vegetation index (NDVI), 1982–2011. Remote Sens. 5, 4799–4818.
Feng, X., Porporato, A., Rodriguez-Iturbe, I., 2013. Changes in rainfall seasonality in the tropics. Nat. Clim. Chang. 3, 811–815.
Fensholt, R., Proud, S.R., 2012. Evaluation of earth observation based global long term vegetation trends—comparing GIMMS and MODIS global NDVI time series. Remote Sens. Environ. 119, 131–147.
Fensholt, R., Rasmussen, K., Nielsen, T.T., Mbow, C., 2009. Evaluation of earth observation based long term vegetation trends—intercomparing NDVI time series trend analysis consistency of Sahel from AVHRR GIMMS, Terra MODIS and SPOT VGT data. Remote Sens. Environ. 113, 1886–1898.
Franch, B., Vermote, E.F., Roger, J.-C., Murphy, E., Becker-Reshef, I., Justice, C., Claverie, M., Nagol, J., Csiszar, I., Meyer, D., 2017. A 30+ year AVHRR land surface reflectance climate data record and its application to wheat yield monitoring. Remote Sens. 9, 296.
Friedl, M.A., Sulla-Menashe, D., Tan, B., Schneider, A., Ramankutty, N., Sibley, A., Huang, X., 2010. MODIS Collection 5 global land cover: algorithm refinements and characterization of new datasets. Remote Sens. Environ. 114, 168–182.
Garonna, I., de Jong, R., de Wit, A.J.W., Mücher, C.A., Schmid, B., Schaepman, M.E., 2014. Strong contribution of autumn phenology to changes in satellite-derived growing season length estimates across Europe (1982–2011). Glob. Chang. Biol. 20, 3457–3470.
Garonna, I., de Jong, R., Schaepman, M.E., 2016. Variability and evolution of global land surface phenology over the past three decades (1982–2012). Glob. Chang. Biol. 22, 1456–1468.
Gitelson, A.A., Kaufman, Y.J., 1998. MODIS NDVI optimization to fit the AVHRR data series—spectral considerations. Remote Sens. Environ. 66, 343–350.
Gonsamo, A., Chen, J.M., Ooi, Y.W., 2018. Peak season plant activity shift towards spring is reflected by increasing carbon uptake by extratropical ecosystems. Glob. Chang. Biol. 24, 2117–2128.
Guan, K., 2013. Hydrological Variability on Vegetation Seasonality, Productivity and Composition in Tropical Ecosystems of Africa. Princeton University.
Guay, K.C., Beck, P.S.A., Berner, L.T., Goetz, S.J., Baccini, A., Buermann, W., 2014. Vegetation productivity patterns at high northern latitudes: a multi-sensor satellite data assessment. Glob. Chang. Biol. 20, 3147–3158.
Helman, D., 2018. Land surface phenology: what do we really 'see' from space? Sci. Total Environ. 618, 665–673.
Holben, B.N., 1986. Characteristics of maximum-value composite images from temporal AVHRR data. Int. J. Remote Sens. 7, 1417–1434.
Huang, M., Piao, S., Janssens, I.A., Zhu, Z., Wang, T., Wu, D., Ciais, P., Myneni, R.B., Peaucelle, M., Peng, S., 2017. Velocity of change in vegetation productivity over northern high latitudes. Nat. Ecol. Evol. 1, 1649–1654.
Huang, K., Xia, J., Wang, Y., Ahlström, A., Chen, J., Cook, R.B., Cui, E., Fang, Y., Fisher, J.B., Huntzinger, D.N., 2018. Enhanced peak growth of global vegetation and its key mechanisms. Nat. Ecol. Evol. 2, 1897–1905.
Jiang, C., Ryu, Y., Fang, H., Myneni, R., Claverie, M., Zhu, Z., 2017. Inconsistencies of interannual variability and trends in long-term satellite leaf area index products. Glob. Chang. Biol. 23, 4133–4146.
Keenan, T.F., Riley, W.J., 2018. Greening of the land surface in the world's cold regions consistent with recent warming. Nat. Clim. Chang. 8, 825–828.

Kern, A., Marjanović, H., Barcza, Z., 2016. Evaluation of the quality of NDVI3g dataset against collection 6 MODIS NDVI in central Europe between 2000 and 2013. Remote Sens. 8, 955.
Latifovic, R., Trishchenko, A.P., Chen, J., Park, W.B., Khlopenkov, K.V., Fernandes, R., Pouliot, D., Ungureanu, C., Luo, Y., Wang, S., 2005. Generating historical AVHRR 1 km baseline satellite data records over Canada suitable for climate change studies. Can. J. Remote. Sens. 31, 324–346.
Marshall, M., Okuto, E., Kang, Y., Opiyo, E., Ahmed, M., 2016. Global assessment of vegetation index and phenology lab (VIP) and global inventory modeling and mapping studies (GIMMS) version 3 products. Biogeosciences 13, 625.
Miura, T., Huete, A., Yoshioka, H., 2006. An empirical investigation of cross-sensor relationships of NDVI and red/near-infrared reflectance using EO-1 Hyperion data. Remote Sens. Environ. 100, 223–236.
Myneni, R.B., Keeling, C., Tucker, C.J., Asrar, G., Nemani, R.R., 1997. Increased plant growth in the northern high latitudes from 1981 to 1991. Nature 386, 698–702.
Pan, N., Feng, X., Fu, B., Wang, S., Ji, F., Pan, S., 2018. Increasing global vegetation browning hidden in overall vegetation greening: insights from time-varying trends. Remote Sens. Environ. 214, 59–72.
Park, T., Chen, C., Macias-Fauria, M., Tømmervik, H., Choi, S., Winkler, A., Bhatt, U.S., Walker, D.A., Piao, S., Brovkin, V., 2019. Changes in timing of seasonal peak photosynthetic activity in northern ecosystems. Glob. Chang. Biol. 25, 2382–2395.
Piao, S., Wang, X., Ciais, P., Zhu, B., Wang, T., Liu, J., 2011. Changes in satellite-derived vegetation growth trend in temperate and boreal Eurasia from 1982 to 2006. Glob. Chang. Biol. 17, 3228–3239.
Pinzon, J.E., Tucker, C.J., 2014. A non-stationary 1981–2012 AVHRR NDVI3g time series. Remote Sens. 6, 6929–6960.
Scheftic, W., Zeng, X., Broxton, P., Brunke, M., 2014. Intercomparison of seven NDVI products over the United States and Mexico. Remote Sens. 6, 1057–1084.
Tian, F., Fensholt, R., Verbesselt, J., Grogan, K., Horion, S., Wang, Y., 2015. Evaluating temporal consistency of long-term global NDVI datasets for trend analysis. Remote Sens. Environ. 163, 326–340.
Tong, X., Tian, F., Brandt, M., Liu, Y., Zhang, W., Fensholt, R., 2019. Trends of land surface phenology derived from passive microwave and optical remote sensing systems and associated drivers across the dry tropics 1992–2012. Remote Sens. Environ. 232, 111307.
Tucker, C.J., 1979. Red and photographic infrared linear combinations for monitoring vegetation. Remote Sens. Environ. 8, 127–150.
Tucker, C.J., Pinzon, J.E., Brown, M.E., Slayback, D.A., Pak, E.W., Mahoney, R., Vermote, E.F., El Saleous, N., 2005. An extended AVHRR 8-km NDVI dataset compatible with MODIS and SPOT vegetation NDVI data. Int. J. Remote Sens. 26, 4485–4498.
Villaescusa-Nadal, J.L., Franch, B., Vermote, E.F., Roger, J.-C., 2019. Improving the AVHRR long term data record BRDF correction. Remote Sens. 11, 502.
Wang, X., Piao, S., Xu, X., Ciais, P., MacBean, N., Myneni, R.B., Li, L., 2015. Has the advancing onset of spring vegetation green-up slowed down or changed abruptly over the last three decades? Glob. Ecol. Biogeogr. 24, 621–631.
Wang, S., Ju, W., Peñuelas, J., Cescatti, A., Zhou, Y., Fu, Y., Huete, A., Liu, M., Zhang, Y., 2019a. Urban− rural gradients reveal joint control of elevated CO 2 and temperature on extended photosynthetic seasons. Nat. Ecol. Evol. 3, 1076–1085.
Wang, X., Xiao, J., Li, X., Cheng, G., Ma, M., Zhu, G., Arain, M.A., Black, T.A., Jassal, R.S., 2019b. No trends in spring and autumn phenology during the global warming hiatus. Nat. Commun. 10, 1–10.
Xu, L., Myneni, R., Chapin iii, F., Callaghan, T., Pinzon, J., Tucker, C., Zhu, Z., Bi, J., Ciais, P., Tømmervik, H., 2013. Temperature and vegetation seasonality diminishment over northern lands. Nat. Clim. Chang. 3, 581–586.
Yin, H., Udelhoven, T., Fensholt, R., Pflugmacher, D., Hostert, P., 2012. How normalized difference vegetation index (ndvi) trendsfrom advanced very high resolution radiometer (AVHRR) and système probatoire d'observation de la terre vegetation (spot vgt) time series differ in agricultural areas: an inner mongolian case study. Remote Sens. 4, 3364–3389.
Zhang, G., Zhang, Y., Dong, J., Xiao, X., 2013. Green-up dates in the Tibetan Plateau have continuously advanced from 1982 to 2011. Proc. Natl. Acad. Sci. 110, 4309–4314.
Zhang, Y., Song, C., Band, L.E., Sun, G., Li, J., 2017. Reanalysis of global terrestrial vegetation trends from MODIS products: Browning or greening? Remote Sens. Environ. 191, 145–155.
Zhou, L., Tucker, C.J., Kaufmann, R.K., Slayback, D., Shabanov, N.V., Myneni, R.B., 2001. Variations in northern vegetation activity inferred from satellite data of vegetation index during 1981 to 1999. J. Geophys. Res. Atmos. 106, 20069–20083.